ACS APPLIED MATERIALS & INTERFACES

Research Article

www.acsami.org

Three-Dimensional Graphene Networks as a New Substrate for Immobilization of Laccase and Dopamine and Its Application in Glucose/O_2 Biofuel Cell

Yijia Zhang,[†] Mi Chu,[†] Lu Yang, Yueming Tan,* Wenfang Deng, Ming Ma, Xiaoli Su, and Qingji Xie*

Key Laboratory of Chemical Biology and Traditional Chinese Medicine Research (Ministry of Education of China), College of Chemistry and Chemical Engineering, Hunan Normal University, Changsha 410081, China

Supporting Information

ABSTRACT: We report here three-dimensional graphene networks (3D-GNs) as a novel substrate for the immobilization of laccase (Lac) and dopamine (DA) and its application in glucose/O_2 biofuel cell. 3D-GNs were synthesized with an Ni^{2+}-exchange/KOH activation combination method using a 732-type sulfonic acid ion-exchange resin as the carbon precursor. The 3D-GNs exhibited an interconnected network structure and a high specific surface area. DA was noncovalently functionalized on the surface of 3D-GNs with 3,4,9,10-perylene tetracarboxylic acid (PTCA) as a bridge and used as a novel immobilized mediating system for Lac-based bioelectrocatalytic reduction of oxygen. The 3D-GNs-PTCA-DA nanocomposite modified glassy carbon electrode (GCE) showed stable and well-defined redox current peaks for the catechol/*o*-quinone redox couple. Due to the mediated electron transfer by the 3D-GNs-PTCA-DA nanocomposite, the Nafion/Lac/3D-GNs-PTCA-DA/GCE exhibited high catalytic activity for oxygen reduction. The 3D-GNs are proven to be a better substrate for Lac and its mediator immobilization than 2D graphene nanosheets (2D-GNs) due to the interconnected network structure and high specific surface area of 3D-GNs. A glucose/O_2 fuel cell using Nafion/Lac/3D-GNs-PTCA-DA/GCE as the cathode and Nafion/glucose oxidase/ferrocence/3D-GNs/GCE as the anode can output a maximum power density of 112 μW cm^{-2} and a short-circuit current density of 0.96 mA cm^{-2}. This work may be helpful for exploiting the popular 3D-GNs as an efficient electrode material for many other biotechnology applications.

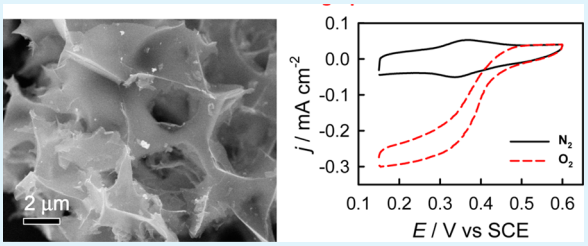

KEYWORDS: *three-dimensional graphene networks, glucose/O_2 biofuel cell, laccase, dopamine, oxygen reduction*

1. INTRODUCTION

Biofuel cells have received much attention in recent years, because they can generate a power source by making use of body fluids and thus serve as an implantable power source.[1−3] The development of effective bioelectrocatalytic system for oxygen reduction reaction is highly desirable for biofuel cells.[4−6] Laccase (Lac) is one of the most commonly considered enzymes for biocathodes in biofuel cells, because it can reduce oxygen directly to water in a four-electron transfer step with the aid of various redox mediators.[5,7,8] The effective immobilization of lac and its mediator on the electrode is the key step to construct a biofuel cell.[4,8,9] Therefore, the development of new electrode material for the immobilization of Lac and its mediator is highly desirable for biofuel cell construction.

Graphene, a two-dimensional (2D) carbon sheet, has been used as one kind of promising materials, due to its special structure and unique properties in chemistry, physics, and mechanics.[10,11] Recently, graphene has been used as a substrate for Lac immobilization for various sensing applications.[12−14] For instance, a bioelectrocatalytic system of graphene integrated with Lac and 2,2-azino-bis(3-ethylbenzothiazoline-6-sulfonic acid) has been developed for detection of the extracellular oxygen released from human erythrocytes.[12] 3D graphene materials have been widely applied in the fields of energy storage, catalysis, environmental protection, stretchable conductors, etc., exhibiting improved performances with respect to 2D graphene materials, because of their large accessible specific surface areas, interconnected conductive network, and special microenvironment.[15−19] Many reports have described the fabrication and attracting properties of 3D graphene; however, the use of 3D graphene for coimmobilization of enzyme and its mediator for biofuel cell application has not been examined to date.

Dopamine (DA) is an important neurotransmitter of redox activity that has attracted extensive studies.[20−23] For instance, DA has been exploited as a mediator in solution and as a surface-bound mediator for biosensor construction.[23−25] As is well-known, Lac can catalyze the oxidation of many phenolic compounds (e.g., catechol) accompanied by the reduction of oxygen.[26−28] DA as a simple organic chemical in the catecholamine family can be oxidized to dopaminequinone

Received: May 7, 2014
Accepted: July 14, 2014
Published: July 14, 2014

with the aid of Lac in the presence of O_2,[29] so the exploitation of DA as an electron mediator of Lac for bioelectrocatalytic reduction of oxygen should be feasible and interesting.

Recently, we have developed a new method to synthesize three-dimensional graphene networks (3D-GNs) using 732-type sulfonic acid ion-exchange resin as carbon precursor.[30] The 3D-GNs showed an interconnected network structure and a high specific surface area. Herein, the 3D-GNs were used as a new substrate for Lac and DA immobilization. DA was noncovalently functionalized on the surface of 3D-GNs with 3,4,9,10-perylene tetracarboxylic acid (PTCA) as a bridge and was used as a novel mediating system for efficient Lac-based bioelectrocatalytic reduction of oxygen. As a result, a glucose/O_2 fuel cell using 3D-GNs-PTCA-DA/Lac/Nafion modified glassy carbon electron (GCE) as a biocathode can output high power density.

2. EXPERIMENTAL SECTION

Chemicals. Lac (*Trametes Versicolor*, 22.3 U mg^{-1}), glucose oxidase (GOx, ~150 U mg^{-1}), and DA hydrochloride were purchased from Sigma-Aldrich. 3,4,9,10-Perylene tetracarboxylic dianhydride was purchased from J&K Chemical Ltd. (Shanghai, China). *N,N′*-Dicyclohexylcarbodiimide (DCC) was purchased from Sinopharm Chemical Reagent Co. Ltd. (Shanghai, China). 2D graphene nanosheets (2D-GNs) were purchased from XFNano Material Tech Co., Ltd. (Nanjing, China). Phosphate buffer solution (PBS, pH 7.0) was prepared with 0.1 M K_2HPO_4−KH_2PO_4. Acetate buffer solution (pH 3.0 or 5.0) was 0.1 M HAc-NaAc aqueous solution. All other chemicals were of analytical grade or better quality. Ultrapure water (Millipore, ≥18 MΩ cm) was used throughout.

Apparatus. Electrochemical experiments were conducted on a CHI760E electrochemical workstation (CH Instrument Co., U.S.A.). A conventional three-electrode system included a GCE, a Pt auxiliary electrode and a saturated calomel reference electrode (SCE). All potentials in this work are referenced to the SCE. The cell voltage (U_{cell}) and the cell current (I_{cell}) of the glucose/O_2 biofuel cell at varying external resistance loads (R_e) were dynamically monitored with the electrochemical noise (ECN) module of the Autolab PGSTAT30 electrochemical workstation.[31,32] Scanning electron microscopy (SEM) studies were performed on a Hitachi S4800 scanning electron microscope. The samples were prepared by dropping ethanol dispersions of the samples onto Pt foils and immediately evaporating the solvent. Transmission electron microscopy (TEM) studies were performed on a TECNAI F-30 high-resolution transmission electron microscope. XRD studies were performed on a PANalytical X'pert Pro X-ray diffractometer. X-ray photoelectron spectroscopy (XPS) was recorded on a PHI QUANTUM 2000 X-ray photoelectron spectroscopic instrument. Surface area and pore size were determined by a surface area and porosity analyzer (Micromeritics Instrument Corp. ASAP2020). Fourier transform infrared (FT-IR) spectra were collected on a Nicolet Nexus 670 FT-IR instrument (Nicolet Instrument Co., U.S.A.) in its transmission mode.

Synthesis of 3D-GNs. The 3D S-GNs were synthesized with an Ni^{2+}-exchange/KOH activation combination method using a 732-type sulfonic acid ion-exchange resin as the carbon precursor.[30] The pretreated 732-type sulfonic acid ion-exchange resin was impregnated with Ni^{2+} in 100 mL nickel acetate solution with concentration of 0.05 M for 8 h. The ion-exchange resin was washed with deionized water and dried at 60 °C in a vacuum oven. The Ni^{2+}-impregnated ion exchanged resin (10 g) was added in a 400 mL KOH/ethanol solution containing 40 g KOH and stirred at 80 °C until the mixture solution became an "ink-paste", followed by another 6 h of static soaking in ambient conditions. Then, the mixture was dried at 70 °C for 60 h and then smashed by a disintegrator. Finally, the mixture was heated at 850 °C for 2 h in N_2 atmosphere, with a heating ratio of 2 °C min^{-1}. Finally, the resulting sample was etched in excessive 0.1 M HCl aqueous solution. The resulting products were collected by centrifugation, washed with deionized water, and finally dried at 60 °C in a vacuum oven for 12 h.

Preparation of 3D-GNs-PTCA-DA. PTCA was prepared from 3,4,9,10-perylene tetracarboxylic dianhydride according to a previous report.[33] For the preparation of 3D-GNs-PTCA, 20 mg of 3D-GNs were ultrasonicated in 100 mL of ethanol containing 40 mg of PTCA for 1 h and stirred continuously for 12 h at room temperature. Then, the mixture was filtered through a nylon membrane (0.22 μm) and washed several times with ethanol and ultrapure water, and finally dried in a vacuum oven at 60 °C. The final product was denoted as 3D-GNs-PTCA. For the preparation of 3D-GNs-PTCA-DA nanocomposite, 10 mg of DCC were dissolved in 60 mL of *N,N′*-dimethylformamide (DMF) under N_2 atmosphere. Then, 40 mL of DMF solution containing 10 mg of 3D-GNs-PTCA was added to the above solution and stirred at 40 °C for 48 h under N_2 atmosphere. The resulting products were collected by filtration and washed with DMF, ethanol, and ultrapure water for several times, and finally dried in a vacuum oven at 60 °C. For comparison, a 2D graphene nanosheets (2D-GNs)-PTCA-DA nanocomposite was also prepared similarly as the 3D-GNs-PTCA-DA except that commercial 2D-GNs were used instead.

Electrode Modifications and Biofuel Cell Construction. One milligram of 3D-GNs, 3D-GNs, 3D-GNs-PTCA-DA, or 2D-GNs-PTCA-DA was dispersed in 1 mL ethanol by sonication, and 2 μL of the above solution was deposited on GCE and dried in air for electrochemical studies. To prepare Nafion/Lac/3D-GNs-PTCA-DA/GCE, 3 μL of Lac aqueous solution (1 mg mL^{-1}) was mixed with 10 μL of the dispersion of 3D-GNs-PTCA-DA nanocomposite described above. Then, 2 μL of the mixture was cast-coated on GCE and dried in air. Nafion solution (2 μL; 0.1 wt %) was placed on the surface of the above electrodes. For comparison, Nafion/Lac/2D-GNs-PTCA-DA/GCE was prepared similarly as the Nafion/Lac/3D-GNs-PTCA-DA/GCE except that commercial 2D-GNs were used instead.

The bioanode was fabricated as follows. Briefly, 2 μL of 1 mg mL^{-1} 3D-GNs was cast on the surface of an GCE, air-dried, followed by successive casting 4 μL of 0.05 M ferrocence (Fc) acetone solution, 2 μ L of 2 mg/mL GOx aqueous solution, and 2 μL of 0.1 wt % Nafion solution, and each casting was done after the previous cast had been air-dried. The as-prepared enzyme electrode was denoted as Nafion/GOx/Fc/3D-GNs/GCE. For comparison, Nafion/GOx/Fc/MWCNTs/GCE was prepared similarly as Nafion/GOx/Fc/3D-GNs/GCE except that MWCNTs were used instead.

The glucose/O_2 biofuel cell was fabricated as follows. Bioanode is the Nafion/GOx/Fc/3D-GNs/GCE, and biocathode is the Nafion/Lac/3D-GNs-PTCA-DA/GCE. The electrolyte is O_2-saturated acetate buffer solution (pH 5.0) containing 10 mM glucose. The performance of the glucose/O_2 biofuel cell was investigated by the ECN device.

3. RESULTS AND DISCUSSION

A 732-type sulfonic acid ion-exchange resin was used as the carbon precursor to synthesize the 3D-GNs.[30] The synthesis of 3D-GNs involves Ni^{2+} impregnation, followed by heat treatment in the presence of KOH, and then acid leaching. The morphologies of the prepared 3D-GNs were examined by SEM and TEM. As shown in Figure 1, the 3D-GNs exhibit an open and interconnected network structure. TEM images clearly reveal that the 3D-GNs are composed of graphene nanosheets. As shown in Figure 1d, high-resolution TEM (HR-TEM) image reveals that the thickness of the few-layer graphene wall is ~4 nm. The lattice fringes clearly show an interplanar spacing of 0.33 nm, consistent with the (002) lattice spacing of graphite. The chemical structure and composition of the 3D-GNs were further studied by XRD, Raman spectroscopy, and XPS. As shown in Figure 2a, a strong peak observed at 26.0° can be attributed to the (002) plane of the hexagonal graphite structure, indicating a high degree of crystallization for the 3D-GNs. Figure 2b shows the Raman spectrum of 3D-GNs.

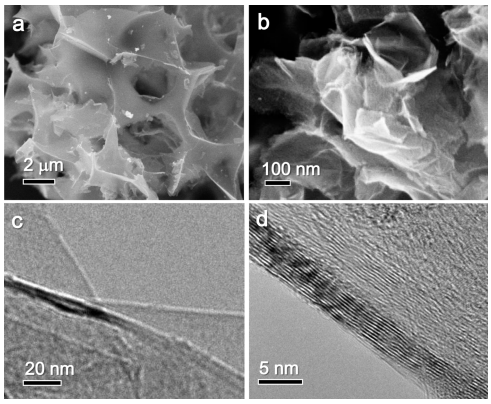

Figure 1. SEM (a, b) and TEM (c, d) images of 3D-GNs.

The peak at 1350 cm^{-1} (D-band) is attributed to the vibration of sp2 hybridized carbon atoms, while the peak at 1580 cm^{-1} (G-band) is attributed to the vibration of sp3 hybridized carbon atoms. The intensity ratio of D-band to G-band (I_D/I_G) can be used evaluate the degree of crystallization. The intensity ratio of D-band to G-band (I_D/I_G) is 0.52, suggesting a high degree of crystallization for the 3D-GNs, well consistent with XRD result. The involvement of S and O in the 3D-GNs was verified by XPS (Supporting Information Figure S1a). The C/S/O atomic ratio is ca. 23:1.3:1.0. The high C/O atomic ratio indicates only a few oxygen-containing functional groups. Supporting Information Figure S1, b and c, shows the high resolution XPS spectra of C 1s and S 2p. The peak at 284.6 eV and the peaks between 286.0 and 290.0 eV are related to the peak of C═C and oxygen-containing groups, respectively. Carbon element mainly exists in the form of C═C, also indicating a high degree of crystallization for the 3D-GNs. The high resolution XPS spectrum of S 2p indicates that sulfur element mainly exists in the form of C−S−C (Supporting Information Figure S1c). Figure 2, c and d, shows the nitrogen adsorption−desorption isotherms and pore size distribution of 3D-GNs. The 3D-GNs show a high Brunauer−Emmett−Teller (BET) surface area of 2153 $m^2\ g^{-1}$. The pore size distribution calculated from desorption data using the Barrett−Joyner−Halenda (BJH) model shows that abundant mesopores exist in the 3D-GNs in the range 2−9 nm. The surface area of the 3D GNs is much higher than that of commercial 2D-GNs (~200 $m^2\ g^{-1}$ given by manufacturer, Supporting Information Figure S2). The high specific surface area is mainly attributed to the formation of mesoporous structure resulting from KOH activation. In fact, KOH activation has been reported to produce abundant micropores and mesopores in carbon materials.[16,34,35] The open and interconnected network structure in combination with the high surface area of 3D-GNs should be beneficial for the immobilization of biomacromolecules and small organic molecules.

3D-GNs were used as a new substrate for DA immobilization. DA was noncovalently functionalized on the surface of 3D-GNs with PTCA as a bridge. With the aid of a pyrenyl group, PTCA can be tightly attached to the surface of 3D-GNs by $\pi-\pi$ stacking interactions. Then, the carboxyl groups of PTCA can react with the amine group of DA in the presence of DCC. Surface modifications of 3D-GNs were characterized by FT-IR spectroscopy. Figure 3 shows the FT-IR spectra of 3D-GNs, 3D-GNs-PTCA, and 3D-GNs-PTCA-DA. In the FT-IR spectrum of 3D-GNs-PTCA, the increased stretching band for C═O at 1750 cm^{-1}, are assigned to the carboxyl groups of PTCA, which indicates the successful functionalization of the 3D-GNs by PTCA via $\pi-\pi$ interactions between the pyrenyl group of PTCA and the 3D-GNs. In the FT-IR spectrum of 3D-GNs-PTCA-DA, the C═O peak at 1750 cm^{-1} assigned to the carboxyl groups of PTCA decreased obviously, and a new

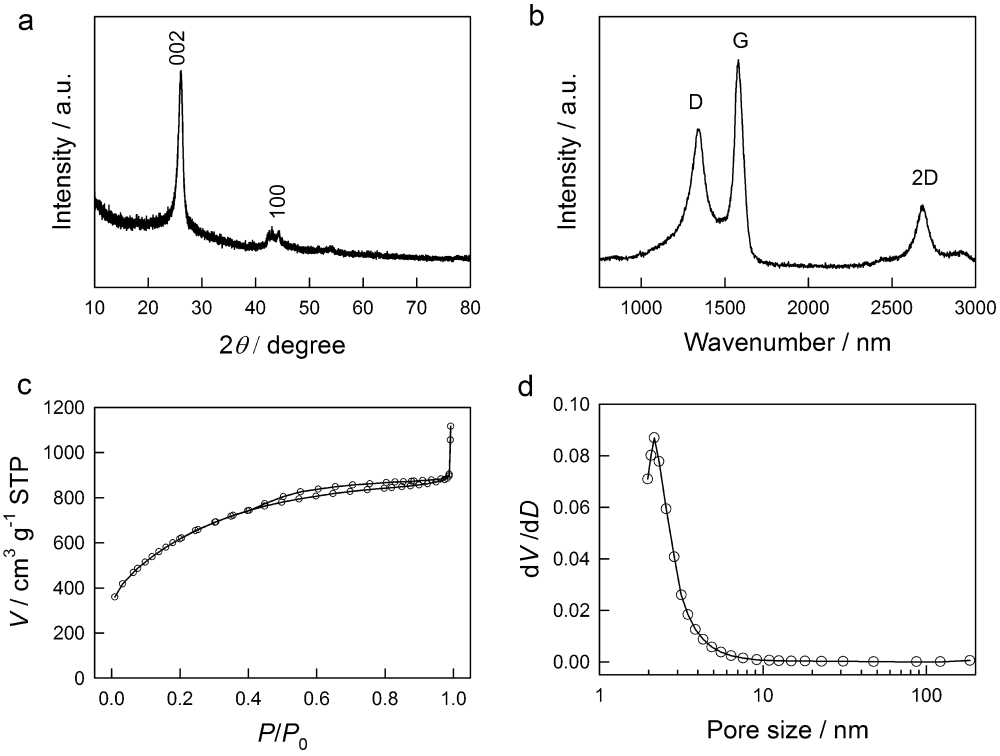

Figure 2. XRD pattern (a), Raman spectrum (b), nitrogen adsorption/desorption isotherms (c), and pore distribution (d) of 3D-GNs.

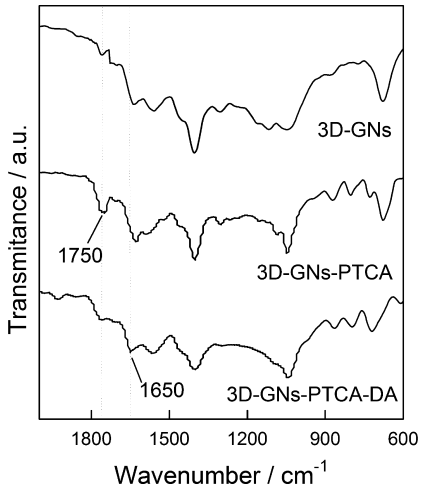

Figure 3. FT-IR spectra of 3D-GNs, 3D-GNs-PTCA, and 3D-GNs-PTCA-DA.

peak at 1650 cm^{-1} for the C═O stretching vibration of acid amide units can be observed, indicating that carboxyl groups have almost been converted to acid amides. Cyclic voltammetry was also used to characterize the surface modification of 3D-GNs. As shown in Supporting Information Figure S3, no obvious redox peak is observed at 3D-GNs/GCE and 3D-GNs-PTCA/GCE in 0.1 M PBS (pH 7.0). There is a new pair of redox peaks centered at 0.23 V with peak-to-peak separation of 20 mV for 3D-GNs-PTCA-DA/GCE, which is associated with the reversible catechol/*o*-quinone redox of the DA moieties (Supporting Information Scheme S1). These results should confirm that DA has been successfully functionalized on the surface of 3D-GNs.

Cyclic voltammograms at scan rate from 5 to 1000 mV s^{-1} were recorded for 3D-GNs-PTCA-DA/GCE (Figure 4a). The voltammetric peak currents were proportional to scan rate (ν) up to 1000 mV s^{-1}, consistent with the surface-type behavior of the system (Figure 4b). The immobilized DA moieties (Γ) can be quantified from the slope of j_p vs ν curve according to the following formula,[36] $j_p = n^2F^2\nu\Gamma/4RT$, where n is the number of electrons transferred, and F is the Faraday constant (96485.3 C mol^{-1}). The interfacial population of DA moieties on 3D-GNs-PTCA-DA/GCE is ca. 7.0×10^{-10} mol cm^{-2}. Commercial 2D-GNs were also used as a substrate for DA immobilization, and a 2D-GNs-PTCA-DA/GCE was prepared similarly as the 3D-GNs-PTCA-DA/GCE except that commercial 2D-GNs were used instead. The interfacial population of DA moieties on the 2D-GNs-PTCA-DA/GCE is only 1.8×10^{-10} mol cm^{-2} (Supporting Information Figure S4), which is much lower than that on the 3D-GNs-PTCA-DA/GCE. The 3D-GNs show much high surface are than 2D-GNs, so more DA molecules can be immobilized on their surface. This result should indicate that the 3D-GNs are a better substrate than 2D-GNs for small molecules immobilization.

The stability of the 3D-GNs-PTCA-DA/GCE in PBS (pH 7.0) was investigated. As shown in Supporting Information Figure S5, the long-term potential cycling at 50 mV s^{-1} for 100 cycles barely resulted in any changes. Cyclic voltammetric behaviors at different solution pH were examined (Figure 4c). Figure 4d shows formal potential ($E^{0\prime}$) as functions of the solution pH. Formal potentials vary linearly with solution pH with a slope of 59.3 mV per pH unit, which is very close to the anticipated Nernstian value of 59.2 mV per pH unit for a two-electron-two-proton electrochemical reaction.

Nafion/Lac/3D-GNs-PTCA-DA/GCE was prepared and used for bioelectrocatalytic reduction of oxygen. Cyclic voltammograms of Nafion/Lac/3D-GNs-PTCA-DA/GCE in

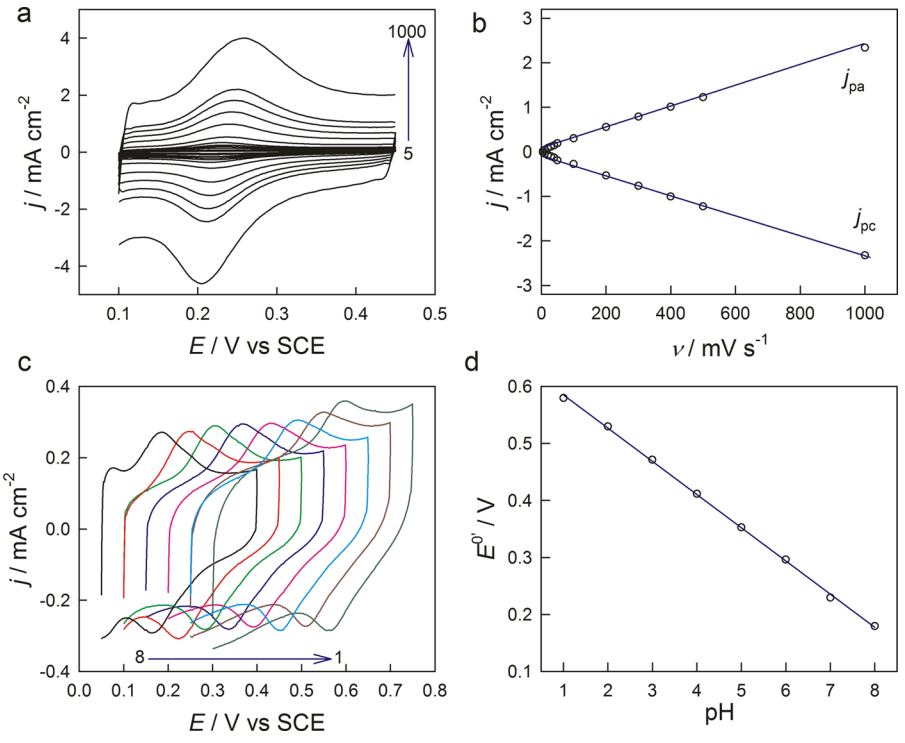

Figure 4. Scan rate dependence of cyclic voltammograms (a) and peak currents (b) of 3D-GNs-PTCA-DA/GCE in 0.1 M PBS (pH 7.0). The pH dependence of cyclic voltammograms (c) and formal potential (d) at 3D-GNs-PTCA-DA/GCE at a scan rate of 50 mVs^{-1}.

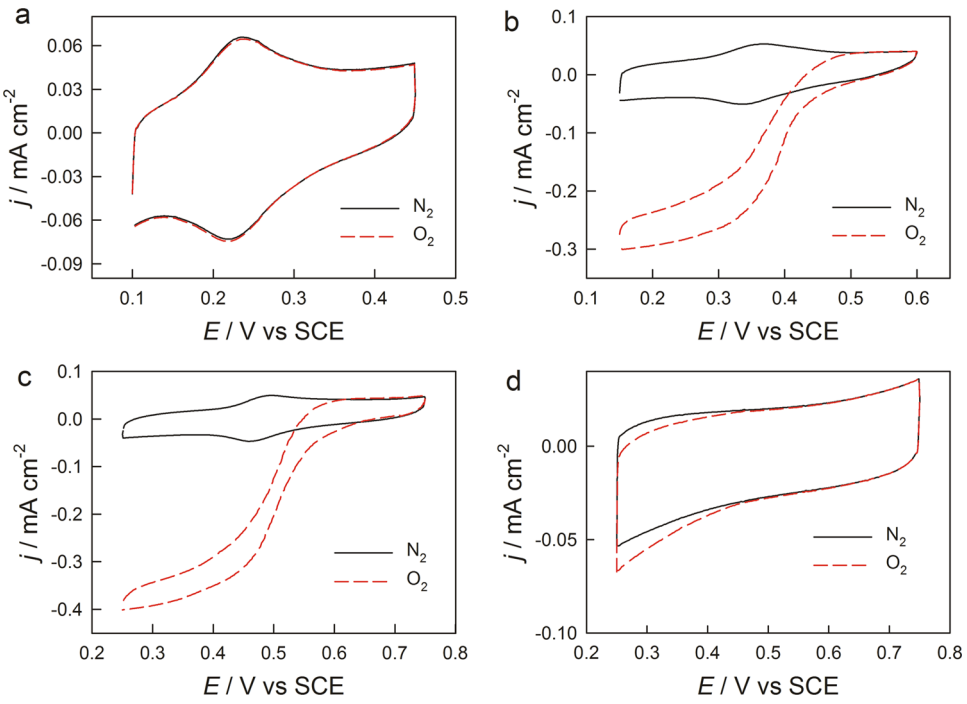

Figure 5. (a–c) Cyclic voltammograms at Nafion/Lac/3D-GNs-PTCA-DA/GCE in N_2 and O_2-saturated buffer solutions at pH 7.0 (a), 5.0 (b) and 3.0 (c). (d) Cyclic voltammograms at Nafion/Lac/3D-GNs/GCE in N_2 and O_2-saturated buffer solution (pH 3.0). Scan rate: 10 mV s^{-1}.

O_2-saturated buffer solutions at different solution pH are shown in Figure 5a–c. In O_2-saturated PBS (pH 7.0), the Nafion/Lac/3D-GNs-PTCA-DA/GCE shows low catalytic activity toward oxygen reduction, because Lac only shows high catalytic activity in acidic solutions. In O_2-saturated acetate buffer solution (pH 5.0), a much larger cathodic current can be observed at Nafion/Lac/3D-GNs-PTCA-DA/GCE, as compared with that recorded in N_2-saturated acetate buffer solution, which is a typical electrocatalytic characteristic. The bioelectrocatalytic reduction of oxygen starts at 0.49 V, and the observed reduction currents increase rapidly during negative potential scanning, indicating that the immobilized DA is an efficient mediating system for Lac. Electron transfer steps for the bioelectrocatalytic reduction of oxygen are shown in Supporting Information Scheme1 S1. Due to the excellence of mediated electron transfer by 3D-GNs-PTCA-DA, the electrons are transferred from the electrode to the T1 copper site of Lac that is the redox canter of Lac, and further to the T2/T3 site that contains 3 Cu ions and is responsible of O_2 reduction to H_2O. In the catalysis cycle, the Lac is oxidized by oxygen and can be turned over by catechol species with production of *o*-quinone species, and catechol species can be regenerated at the electrode, thus the whole catalysis cycle solely consumes oxygen (Supporting Information Scheme S2). The onset potential for oxygen reduction at pH 3.0 shifts positively to 0.61 V, and the cathodic current is even larger than that at pH 5.0. In fact, Lac has been reported to show its largest catalytic activity at pH 3.0.[27,37] As shown in Supporting Information Figure S6, the 3D-GNs/GCE and 3D-GNs-PTCA-DA/GCE showed low electrocatalytic activity toward oxygen reduction in O_2-saturated buffer solution (pH 3.0). These results highlight the advantage of Lac-based bioelectrocatalytic reduction of oxygen. It is reported that direct electron transfer between the redox sites of Lac and the electrode can be achieved by modifying nanoelements (e.g., Au nanoparticles) on electrode surface.[5,38] To study the direct electron transfer between the redox sites of Lac and the electrode, Nafion/Lac/3D-GNs/GCE was prepared similarly as Nafion/Lac/3D-GNs-PTCA-DA/GCE except the absence of PTCA-DA. As shown in Figure 5d, the electrocatalytic current of Nafion/Lac/3D-GNs/GCE is much lower than that of Nafion/Lac/3D-GNs-PTCA-DA/GCE, highlighting the excellence of mediated electron transfer by 3D-GNs-PTCA-DA nanocomposite. In fact, direct electron transfer requires a short distance (less than 15–20 Å) between the redox center of the immobilized enzyme molecules and the electrode surface, which is not straightforward in many cases.[5] Thus, it is reasonable that the Nafion/Lac/3D-GNs/GCE shows low catalytic activity toward oxygen reduction. For comparison, Nafion/Lac/2D-GNs-PTCA-DA/GCE was prepared and used for bioelectrocatalytic reduction of oxygen. As shown in Supporting Information Figure S7, the electrocatalytic current of the Nafion/Lac/2D-GNs-PTCA-DA/GCE is much lower than that of Nafion/Lac/3D-GNs-PTCA-DA/GCE, indicating that the 3D-GNs are better substrate for Lac and its mediator immobilization.

The glucose oxidation at Nafion/GOx/Fc/3D-GNs/GCE and Nafion/GOx/Fc/MWCNTs/GCE was studied in acetate buffer solution (pH 5.0). As shown in Supporting Information Figure S8, a pair of well-defined redox peaks at 0.18 V for Fc immobilized on 3D-GNs was observed in acetate buffer solution (pH 5.0) without glucose, and obvious anodic catalytic current was observed in the presence of 10 mM glucose. The electrocatalytic current of the Nafion/GOx/Fc/3D-GNs/GCE is larger than that of the Nafion/GOx/Fc/MWCNTs/GCE, because the interconnected network structure in combination with the high surface area of 3D-GNs is beneficial for immobilizing more GOx and Fc. Thus, the Nafion/GOx/Fc/3D-GNs/GCE was used as the bioanode to assemble the glucose/O_2 biofuel cell. The glucose/O_2 biofuel cell was carried out at pH 5.0 for convenience, because the catalytic activity of Lac from *T. versicolor* toward O_2 reduction increased but that of GOx toward glucose oxidation decreased with pH decrease

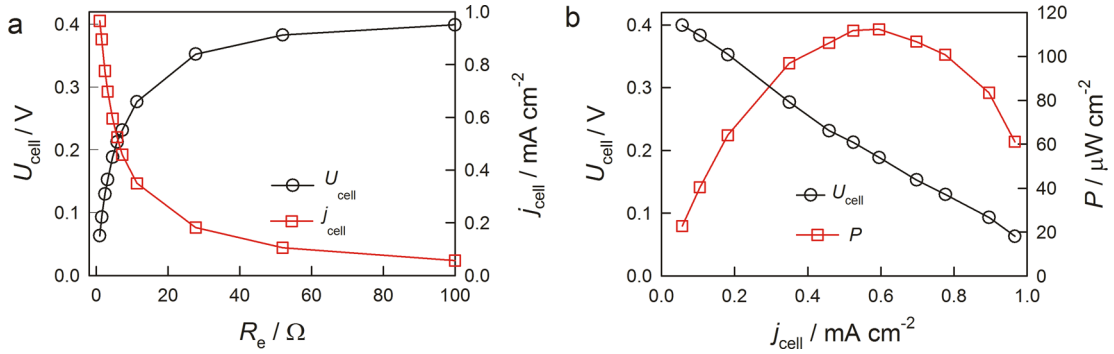

Figure 6. U_{cell} and j_{cell} as functions of external load (a) as well as j_{cell} and P as functions of j_{cell} (b) for the glucose/O_2 biofuel cell.

from 7.0 to 3.0.[27,39,40] Electron transfer steps at the bioanode and the biocathode of the assembled glucose/O_2 biofuel cell are shown in Supporting Information Scheme S2. Figure 6a shows U_{cell} and j_{cell} of the biofuel cell operating in acetate buffer solution (pH 5.0) containing 10 mM glucose at varying R_e. With the increase in R_e, U_{cell} increased and reached 0.40 V at 100 KΩ, while j_{cell} decreased from 0.96 mA cm^{-2} to 57 μA cm^{-2}. Figure 6b shows U_{cell} and the power density (P) of the glucose/O_2 biofuel cell as functions of U_{cell} at these R_e. The maximum P is 112 μW cm^{-2} at 0.19 V, which is higher than most glucose biofuel cells reported previously (Supporting Information Table S1). Supporting Information Figure S9 shows the current density response of the glucose/O_2 biofuel cell continuously operating at 100 k Ω for 72 h. The glucose/O_2 biofuel cell still retained ~84% of its initial current density after 72-h continuous discharging, indicating that the enzymes entrapped in the 3D-GNs possess high stability. This result indicates that the 3D-GNs are a promising substrate for enzymatic activity retention.

4. CONCLUSIONS

In summary, novel 3D-GNs with interconnected pore structure and high surface area were synthesized and used as a new substrate for the immobilization of Lac and DA for bioelectrocatalytic reduction of oxygen. The Nafion/Lac/3D-GNs-PTCA-DA/GCE showed high catalytic activity for oxygen reduction, due to the excellence of mediated electron transfer by 3D-GNs-PTCA-DA nanocomposite. Moreover, the Nafion/Lac/3D-GNs-PTCA-DA/GCE exhibited much higher electrocatalytic activity than the Nafion/Lac/2D-GNs-PTCA-DA/GCE, indicating that the 3D-GNs are better substrate for Lac and its mediator immobilization. The glucose/O_2 fuel cell using the Nafion/Lac/3D-GNs-PTCA-DA/GCE as the cathode can output high power density, suggesting a promising biocathode for glucose/O_2 fuel cell application. The 3D-GNs may be extended to the immobilization of many other biomolecules for wide biotechnology applications.

■ ASSOCIATED CONTENT

Ⓢ Supporting Information

Additional scheme and figures. This material is available free of charge via the Internet at http://pubs.acs.org.

■ AUTHOR INFORMATION

Corresponding Authors

*Email: tanyueming0813@126.com.
*Email: xieqj@hunnu.edu.cn.

Author Contributions

†Y.Z. and M.C. contributed equally to this work.

Notes

The authors declare no competing financial interest.

■ ACKNOWLEDGMENTS

This work is supported by NSFC (21305041, 21175042, 20975038, and 21275052), Scientific Research Fund of Hunan Provincial Education Department (13B063), Program for Science and Technology Innovative Research Team in Higher Educational Institutions of Hunan Province, and Start-Up Fund for Young Teachers in Hunan Normal University.

■ REFERENCES

(1) Barton, S. C.; Gallaway, J.; Atanassov, P. Enzymatic Biofuel Cells for Implantable and Microscale Devices. *Chem. Rev.* **2004**, *104*, 4867−4886.
(2) Halámkova, L.; Halámek, J.; Bocharova, V.; Szczupak, A.; Alfonta, L.; Katz, E. Implanted Biofuel Cell Operating in a Living Snail. *J. Am. Chem. Soc.* **2012**, *134*, 5040−5043.
(3) Szczupak, A.; Halámek, J.; Halámková, L.; Bocharova, V.; Alfontac, L.; Katz, E. Living Battery-Biofuel Cells Operating In Vivo in Clams. *Energy Environ. Sci.* **2012**, *5*, 8891−8895.
(4) Karnicka, K.; Miecznikowski, K.; Kowalewska, B.; Skunik, M.; Opallo, M.; Rogalski, J.; Schuhmann, W.; Kulesza, P. J. ABTS-Modified Multiwalled Carbon Nanotubes as an Effective Mediating System for Bioelectrocatalytic Reduction of Oxygen. *Anal. Chem.* **2008**, *80*, 7643−7648.
(5) Gutiérrez-Sánchez, C.; Pita, M.; Vaz-Domínguez, C.; Shleev, S.; De Lacey, A. L. Gold Nanoparticles as Electronic Bridges for Laccase-Based Biocathodes. *J. Am. Chem. Soc.* **2012**, *134*, 17212−17220.
(6) Mano, N.; Fernandez, J. L.; Kim, Y.; Shin, W.; Bard, A. J.; Heller, A. Oxygen Is Electroreduced to Water on a "Wired" Enzyme Electrode at a Lesser Overpotential than on Platinum. *J. Am. Chem. Soc.* **2003**, *125*, 15290−15291.
(7) Solomon, E. I.; Sundaram, U. M.; Machonkin, T. E. Multicopper Oxidases and Oxygenases. *Chem. Rev.* **1996**, *96*, 2563−2606.
(8) Soukharev, V.; Mano, N.; Heller, A. A Four-Electron O_2-Electroreduction Biocatalyst Superior to Platinum and a Biofuel Cell Operating at 0.88 V. *J. Am. Chem. Soc.* **2004**, *126*, 8368−8369.
(9) Gallaway, J. W.; Barton, S. A. C. Kinetics of Redox Polymer-Mediated Enzyme Electrodes. *J. Am. Chem. Soc.* **2008**, *130*, 8527−8536.
(10) Novoselov, K. S.; Geim, A. K.; Morozov, S. V.; Jiang, D.; Zhang, Y.; Dubonos, S. V.; Grigorieva, I. V.; Firsov, A. A. Electric Field Effect in Atomically Thin Carbon Films. *Science* **2004**, *306*, 666−669.
(11) Allen, M. J.; Tung, V. C.; Kaner, R. B. Honeycomb Carbon: A Review of Graphene. *Chem. Rev.* **2010**, *110*, 132−145.
(12) Wu, X.; Hu, Y.; Jin, J.; Zhou, N.; Wu, P.; Zhang, H.; Cai, C. Electrochemical Approach for Detection of Extracellular Oxygen Released from Erythrocytes Based on Graphene Film Integrated with

Laccase and 2,2-Azino-bis(3-ethylbenzothiazoline-6-sulfonic Acid). *Anal. Chem.* **2010**, *82*, 3588−3596.
(13) Oliveira, T. M. B. F.; Barroso, M. F.; Morais, S.; Araújo, M.; Freire, C.; Lima-Neto, P. d.; Correia, A. N.; Oliveira, M. B. P. P.; Delerue-Matos, C. Laccase-Prussian Blue Film-Graphene Doped Carbon Paste Modified Electrode for Carbamate Pesticides Quantification. *Biosens. Bioelectron.* **2013**, *47*, 292−299.
(14) Eremia, S. A.; Vasilescu, I.; Radoi, A.; Litescu, S. C.; Radu, G. L. Disposable Biosensor Based on Platinum Nanoparticles-Reduced Graphene Oxide-Laccase Biocomposite for the Determination of Total Polyphenolic Content. *Talanta* **2013**, *110*, 164−170.
(15) Chen, Z.; Ren, W.; Gao, L.; Liu, B.; Pei, S.; Cheng, H.-M. Three-Dimensional Flexible and Conductive Interconnected Graphene Networks Grown by Chemical Vapor Deposition. *Nat. Mater.* **2011**, *10*, 424−428.
(16) Li, Y.; Li, Z.; Shen, P. K. Simultaneous Formation of Ultrahigh Surface Area and Three-Dimensional Hierarchical Porous Graphene-Like Networks for Fast and Highly Stable Supercapacitors. *Adv. Mater.* **2013**, *25*, 2474−2480.
(17) Meng, Y. N.; Zhao, Y.; Hu, C. G.; Cheng, H. H.; Hu, Y.; Zhang, Z. P.; Shi, G. Q.; Qu, L. T. All-Graphene Core-Sheath Microfibers for All-Solid-State, Stretchable Fibriform Supercapacitors and Wearable Electronic Textiles. *Adv. Mater.* **2013**, *25*, 2326−2331.
(18) Huang, C.; Bai, H.; Li, C.; Shi, G. A Graphene Oxide/Hemoglobin Composite Hydrogel for Enzymatic Catalysis in Organic Solvents. *Chem. Commun.* **2011**, *47*, 4962−4964.
(19) Niu, Z.; Chen, J.; Hng, H. H.; Ma, J.; Chen, X. A Leavening Strategy to Prepare Reduced Graphene Oxide Foams. *Adv. Mater.* **2012**, *24*, 4144−4150.
(20) Schwarz, M. A.; Hauser, P. C. Chiral On-Chip Separations of Neurotransmitters. *Anal. Chem.* **2003**, *75*, 4691−4695.
(21) Xiang, L.; Lin, Y.; Yu, P.; Su, L.; Mao, L. Laccase-Catalyzed Oxidation and Intramolecular Cyclization of Dopamine: A New Method for Selective Determination of Dopamine with Laccase/Carbon Nanotube-based Electrochemical Biosensors. *Electrochim. Acta* **2007**, *52*, 4144−4152.
(22) Li, Y.; Liu, M.; Xiang, C.; Xie, Q.; Yao, S. Electrochemical Quartz Crystal Microbalance Study on Growth and Property of the Polymer Deposit at Gold Electrodes During Oxidation of Dopamine in Aqueous Solutions. *Thin Solid Films* **2006**, *497*, 270−278.
(23) Ge, B.; Tan, Y.; Xie, Q.; Ma, M.; Yao, S. Preparation of Chitosan−Dopamine−Multiwalled Carbon Nanotubes Nanocomposite for Electrocatalytic Oxidation and Sensitive Electroanalysis of NADH. *Sens. Actuators B* **2009**, *137*, 547−554.
(24) Zen, J. M.; Lo, C. W.; Chen, P. J. An Enzymatic Clay-Modified Electrode for Aerobic Glucose Monitoring with Dopamine as Mediator. *Anal. Chem.* **1997**, *69*, 1669−1673.
(25) Degrand, C.; Miller, L. L. An Electrode Modified with Polymer-Bound Dopamine which Catalyzes NADH Oxidation. *J. Am. Chem. Soc.* **1980**, *102*, 5728−5732.
(26) Liu, Y.; Qu, X.; Guo, H.; Chen, H.; Liu, B.; Dong, S. Facile Preparation of Amperometric Laccase Biosensor with Multifunction Based on the Matrix of Carbon Nanotubes−Chitosan Composite. *Biosens. Bioelectron.* **2006**, *21*, 2195−2201.
(27) Tan, Y.; Deng, W.; Ge, B.; Xie, Q.; Huang, J.; Yao, S. Biofuel Cell and Phenolic Biosensor Based on Acid-Resistant Laccase-Glutaraldehyde Functionalized Chitosan−Multiwalled Carbon Nanotubes Nanocomposite Film. *Biosens. Bioelectron.* **2009**, *24*, 2225−2231.
(28) Vianello, F.; Cambria, A.; Ragusa, S.; Cambria, M. T.; Zennaro, L.; Rigo, A. A High Sensitivity Amperometric Biosensor Using a Monomolecular Layer of Laccase as Biorecognition Element. *Biosens. Bioelectron.* **2004**, *20*, 315−321.
(29) Tan, Y.; Deng, W.; Li, Y.; Huang, Z.; Meng, Y.; Xie, Q.; Ma, M.; Yao, S. Polymeric Bionanocomposite Cast Thin Films with In Situ Laccase-Catalyzed Polymerization of Dopamine for Biosensing and Biofuel Cell Applications. *J. Phys. Chem. B* **2010**, *114*, 5016−5024.
(30) Zhang, Y.; Chu, M.; Yang, L.; Deng, W.; Tan, Y.; Ma, M.; Xie, Q. Synthesis and Oxygen Reduction Properties of Three-Dimensional Sulfur-Doped Graphene Networks. *Chem. Commun.* **2014**, *50*, 6382−6385.
(31) Tan, Y.; Xie, Q.; Huang, J.; Duan, W.; Ma, M.; Yao, S. Study on Glucose Biofuel Cells Using an Electrochemical Noise Device. *Electroanalysis* **2008**, *20*, 1599−1606.
(32) Chu, M.; Zhang, Y.; Yang, L.; Tan, Y.; Deng, W.; Ma, M.; Su, X.; Xie, Q.; Yao, S. A Compartment-Less Nonenzymatic Glucose−Air Fuel Cell with Nitrogen-Doped Mesoporous Carbons and Au Nanowires as Catalysts. *Energy Environ. Sci.* **2013**, *6*, 3600−3604.
(33) Zhao, Y.; Zhang, X.; Li, D.; Liu, D.; Jiang, W.; Han, C.; Shi, Z. Water-Soluble 3,4:9,10-Perylene Tetracarboxylic Ammonium as a High-Performance Fluorochrome for Living Cells Staining. *Luminescence* **2009**, *24*, 140−143.
(34) Zhu, Y.; Murali, S.; Stoller, M. D.; Ganesh, K. J.; Cai, W.; Ferreira, P. J.; Pirkle, A.; Wallace, R. M.; Cychosz, K. A.; Thommes, M.; Su, D.; Stach, E. A.; Ruoff, R. S. Carbon-Based Supercapacitors Produced by Activation of Graphene. *Science* **2011**, *332*, 1537−1541.
(35) Zhang, L. L.; Zhao, X.; Stoller, M. D.; Zhu, Y.; Ji, H.; Murali, S.; Wu, Y.; Perales, S.; Clevenger, B.; Ruoff, R. S. Highly Conductive and Porous Activated Reduced Graphene Oxide Films for High-Power Supercapacitors. *Nano Lett.* **2012**, *12*, 1806−1812.
(36) Laviron, E. Adsorption Autoinhibition and Autocatalysis in Polarography and Linear Potential Sweep Voltammetry. *J. Electroanal. Chem.* **1974**, *52*, 355−393.
(37) Tayhas, G.; Palmore, R.; Kim, H. H. Electro-enzymatic Reduction of Dioxygen to Water in the Cathode Compartment of a Biofuel Cell. *J. Electroanal. Chem.* **1999**, *464*, 110−117.
(38) Dagys, M.; Haberska, K.; Shleev, S.; Arnebrant, T.; Kulys, J.; Ruzgas, T. Laccase-Gold Nanoparticle Assisted Bioelectrocatalytic Reduction of Oxygen. *Electrochem. Commun.* **2010**, *12*, 933−935.
(39) Liu, Y.; Wang, M. K.; Zhao, F.; Liu, B. F.; Dong, S. J. A Low-Cost Biofuel Cell with pH-Dependent Power Output Based on Porous Carbon as Matrix. *Chem.—Eur. J.* **2005**, *11*, 4970−4974.
(40) Brunel, L.; Denele, J.; Servat, K.; Kokoh, K. B.; Jolivalt, C.; Innocent, C.; Cretin, M.; Rolland, M.; Tingry, S. Oxygen Transport through Laccase Biocathodes for a Membrane-less Glucose/O_2 Biofuel Cell. *Electrochem. Commun.* **2007**, *9*, 331−336.